Osteogenic and Fluorescent Characterization of Pig-Derived Mesenchymal Stem Cells Between eGFP Transgenesis and Non-viral Plasmid Transfection

Ming-Kai Hsieh
Chang Gung Memorial Hospital
Chia-Jung Wu
Chang Gung Memorial Hospital
Chi-Yun Wang
Chang Gung Memorial Hospital
Tsung-Ting Tsai
Chang Gung Memorial Hospital
Chi-Chien Niu
Chang Gung Memorial Hospital
Po-Liang Lai
Chang Gung Memorial Hospital
Shinn-Chih Wu (✉ scw01@ntu.edu.tw)
National Taiwan University https://orcid.org/0000-0001-8881-1550

Research

Keywords: mesenchymal stem cell, bone regeneration, enhanced green fluorescent, pig

Posted Date: May 12th, 2020

DOI: https://doi.org/10.21203/rs.3.rs-24807/v1

Abstract

Background

Widely used in recent years, mesenchymal stem cells (MSCs) expressing enhanced green fluorescent protein (eGFP) can be tracked during migration to injury sites, while also supporting tri-lineage differentiation. However, the relationship between the expression of green fluorescence and the magnitude of osteogenic differentiation is not clearly defined. Despite increasing use of eGFP-MSCs derived from the transgenic pigs and non-viral eGFP plasmid transfected MSCs in recent years, it remains unclear which cells are suitable for tracking during osteogenic differentiation, and whether the transfected plasmid alters osteogenic potential.

Methods

We compared the expression of green fluorescence and the magnitude of osteogenic differentiation between eGFP MSCs from a transgenic pig (group 1) and non-virally transfected eGFP-MSCs using *trans*IT®-2020 (group 2). Non-transfected MSCs were used as control group (group 3). We also use a scaffold to compare the osteogenic induction environments created by 2-D monolayer cultures and 3-D cultures, respectively

Results

In the monolayer culture, flow cytometry from day 7 to day 28 showed that the percentage of green fluorescent cells in groups 1 and 2 were 99.6% and 59.7% of total cell counts, respectively. Quantification showed that eGFP expression peaked on day 7, decreased after day 14, and plateaued to day 28 in group 1 and group 2. Significant aggregation of eGFP over bone-like nodules was appreciated in group 1. In 3-D culture, eGFP expression increased from day 7 to day 28 in both groups, and was higher in group 1 than in group 2 at each time point. Osteogenic profiles and immunohistochemistry showed more significant osteogenic activity in group 1 and group 3 than in group 2.

Conclusions

The expression of eGFP in the test groups did not significantly change after osteogenic induction. However, quantification data was different in monolayer and 3-D cultures due to spatial limitations, differing extracellular environments, and heterogeneous cell morphology and methods of division. Osteogenic profiles and immunohistochemistry data confirmed that osteogenic potential did not change in transgenic pig-derived MSCs. However osteogenic potential decreased in pig MSCs (pig MSCs) treated with the transfection reagent, likely from related toxicity.

Background

Mesenchymal stem cells (MSCs), a heterogeneous population of stromal cells capable of migrating to the site of injury and supporting tri-lineage differentiation, have been widely studied in recent years.(1)(2)

Thus, researchers believe that MSCs represent an ideal prospect in cell-based tissue engineering strategies.(3) However, studies have been hindered by limited ability to track the progeny and the engraftments of MSCs after osteogenic differentiation.

Enhanced green fluorescent protein (eGFP) exhibits fluorescence in living cells, which allows for *in situ* monitoring in the live animal.(4)(5) The fluorescent signal emitted from eGFP can be detected with optical imaging, fluorescence microscopy, or flow cytometry.(6) This tracking property of eGFP has been widely used for *in vitro* investigations with living cells and has been experimentally tested *in vivo* to track the distribution of transplanted cells in the brain, the liver, the muscle, and the retina.(7)(8)(9)

Establishing efficient, stable cell lines with an integrated eGFP gene is difficult, therefore cells from eGFP transgenic pigs may prove more useful and easier to culture(10). The CAG hybrid promoter-driven eGFP-MSCs derived from the transgenic pigs have been proven to express homogeneous surface epitopes and possess classic trilineage differentiation potential into osteogenic, adipogenic, and chondrogenic lineages with stable, robust EGFP expression in all differentiated progeny.(10) However, demanding techniques such as pronuclear microinjection, expensive breeding and equipment have limited the popularity of eGFP MSCs from transgenic pigs(11,12).

Another easy and safe method to obtain the MSC exhibit GFP fluorescence would be from *in vitro* non-viral transfection of eGFP-encoding plasmid. *Trans*IT®-2020 transfection reagent has shown high performance at lower doses, and therefore less toxicity to cells(13)(14). It is a broad-spectrum reagent that provides exceptional

integration of plasmid DNA into mammalian cells and primary cells, which are typically not easy to transfect(15)(16)(17)(18) . To the best of the authors' knowledges, there is no clear answer in regard to which cells are suitable for tracking during osteogenic differentiation. It is also unclear whether the transfected plasmid will alter the cell's osteogenic potential.

The first aim of the study was to investigate the expression of green fluorescence and the magnitude of osteogenic differentiation between transgenic pig-derived eGFP MSCs and non-viral eGFP transfected MSCs. The second aim is to characterize how the magnitudes of fluorescence and osteogenic differentiation differ between monolayer culture and a simulated *in vitro* 3-D culture.

Methods

Cells culture of MSCs from transgenic pigs

This study was carried out in strict accordance to the Guide for the Care and Use of Laboratory Animals of the National Institutes of Health. All animal cells were retrieved under the approved animal protocols by the Institutional Animal Care and Use Committee of National Taiwan University (NTU107-EL-00128).

Cells in the study were divided into three groups: Group 1, enhanced green fluorescent protein pig MSCs (eGFP-pMSCs) from transgenic pigs (n=6); Group 2, *in vitro* eGFP plasmid transfected pig MSCs (n=6); and Group 3, pig MSCs without transfection (n=6).

In Group 1, passage-12 eGFP-pMSCs from the Department of Animal Science and Technology in National Taiwan University were cultured in minimum essential medium alpha (MEM-α) (Gibco) supplemented with 10% fetal bovine serum (Hyclone) and antibiotic solutions (100 U/mL penicillin, 100 μg/mL streptomycin, 50 μg/mL gentamicin and 250 ng/mL fungizone) (Gibco). The cells were maintained in a humidified 37°C incubator supplied with 5% CO_2.

Isolation and culture of pig mesenchymal stem cells

In group 2 and group 3, bone marrow aspirates of pig mesenchymal stem cell (pMSCs) were obtained from adult domestic pigs (age 15 months; weight 120 kg) from the Department of Animal Science, National Taiwan University (Taipei, Taiwan). Anesthesia was induced with ketamine (10 mg/kg of BW, Sigma-Aldrich, St. Louis, MO) and maintained with inhalation of anesthetic halothane (Sigma-Aldrich, St. Louis, MO). The tibial area was prepared and sterilized, and approximately 5 mL of bone marrow was aspirated into a syringe containing 6,000 U of heparin. Bone marrow mononuclear cells were obtained by negative immunodepletion of $CD3^+$, $CD14^+$, $CD19^+$, $CD38^+$, $CD66b^+$, and glycophorin A^+ cells using a commercially available kit (RosetteSep, Stem Cell Technologies, Vancouver, British Columbia, Canada), according to the manufacturer's instructions. After a 20-minute incubation at room temperature, the cell-antibody mixture was diluted with twice the volume of phosphate- buffered saline (PBS) supplemented with 2% fetal bovine serum (FBS; Hyclone, Logan, UT) and 1 mM EDTA (Invitrogen), layered over an equal volume of Ficoll-Paque medium (1.077 g/cm 3; Amersham Bioscience), and centrifuged at 300 × g for 30 minutes at room temperature. Enriched cells were harvested from the buffer coat and washed twice with control medium, consisting of minimum essential medium (MEM) α (Sigma-Aldrich) supplemented with 20% FBS (Hyclone), 2 mM l-glutamine (Invitrogen), 100 U/mL of penicillin, and 100 μg/mL of streptomycin (Invitrogen). The cells were maintained in a humidified 37 °C incubator supplied with 5% CO_2 as group 1.

Quantitative assessment of cell viability after transfection

In group 2, plasmid enhanced green fluorescent protein gene (pEGFP-N1) was transfected into pMSCs with *Trans*IT®-2020 (Mirus, Madison, WI, USA) according to the manufacturer's instructions. For the cell viability experiments, we prepared *Trans*IT®-2020/pEGFP pMSCs in 6-well plates, removed the growth medium and washed them with one time PBS. On day 1, the cells were transfected with different ratios of transIT-2020: pEGFP-N1 in 1:1, 2:1, 3:1 and 4:1. Either 1 μg or 2.5

μg of pEGFP-N1 were compared. On days 2, 3 and 4, 800 μL of growth medium and

20 μL of cell counting kit-8 (CCK-8; Enzo Life Sciences, East Farmingdale, NY, USA)

solution was added to each well of the plate. The plate was then incubated for 1 hour

37 °C in 5% CO_2. Absorbance was measured at 450 nm using a microplate reader

(TECAN-Infinite 200 PRO, New Taipei City, Taiwan).

In vitro transfection efficiency of pMSCs

The pMSCs were seeded onto 6-well plates at a density of 1×10^6 cells/well and cultivated in 2 mL of DMEM with 10% FBS on day 0. On day 1, the cells were treated with different ratios of *Trans*IT®-2020 and pEGFP-N1. After days 2, 3 and 4, the pMSCs were harvested and mixed with 200 μL of 4% paraformaldehyde on ice for 15 minutes. The pMSCs were then centrifuged at 1500 rpm for 5 minutes at 4°C and re-suspended with 300 μL of PBS in round bottom tubes (Corning Inc. Kennebunk, ME, USA). The expression of GFP in the cells were examined using a fluorescence-activated cell sorting (FACS) Calibur flow cytometer (Becton Dickinson, Heidelberg, Germany). The transfection rate was evaluated using Becton Dickinson Cell Quest software. Different proportions of reagent and plasmid were tested to obtain the highest transfection concentration.

Fluorescence evaluated by image and FACS after osteo-induction in monolayers

To promote cell differentiation, all groups received 0.5 mL/well of osteogenic induction medium (OIM). The OIM medium was composed of complete MEM-α medium enriched with 10^{-7} M dexamethasone (Sigma), 10 mM β-glycerophosphate (Sigma) and 50 μg/mL ascorbic acid (Sigma).(19)(20) The OIM medium was replenished every two or three days for a total of 7 days.

Fluorescent imaging and quantification in monolayers

Three groups of pMSCs were seeded at a density of 1×10^5 cells/well onto 48-well plates, and cultured in 2 mL of DMEM with 10% FBS. After treatment with OIM for a total of 7 days, fluorescent microscopy was acquired on a BioRad MRC 600 microscope from day 7 to day 28. Dishes were washed twice with PBS, fixed in 4% v/v formaldehyde (methanol-free; Polyscience) for 15 minutes, permeabilized with 0.1% v/v Triton X-100 for 5 minutes, and incubated in 10 mg/mL bovine serum albumin and 100 g/mL RNAse for 45 minutes at room temperature. F-actin filaments were stained with Alexafluor-conjugated phalloidin (Molecular Probes) for 20 minutes and nuclei were counter-stained with 10 g/mL propidium iodide (Sigma) for 10 minutes. Finally, samples were washed with PBS and mounted in Vectashield®. The quantitative distribution of the green fluorescent cells was analyzed using NIH Image J software (National Institutes of Health, USA) and presented as the modified integrated density (Modified IntDen). The modified integrated density was calculated based on the following equation: [Selected Integrated

Density - (Area of Selected Cell × Mean Fluorescence of Background Beadings])(19). The images merged form light microscope and fluorescent microscope samples were also investigated.

Flow cytometry analysis of pMSCs in monolayer culture

After treatment with OIM for a total of 7 days, all staining procedures were conducted in non-adherent, round-bottom 48-well plates. Cells in the staining buffer were transferred to each well for corresponding antibodies and for controls including an unstained sample and an isotype control antibody. Samples were transferred to polystyrene FACS tubes (Thermo Fischer) and washed twice by centrifuging at 350g for 5 min and resuspending in 4 mL of PBS (Gibco). Cells were finally resuspended in 250 mL of PBS and retained on ice with protection from light until flow cytometry analysis. Flow cytometry was performed on a FACS Calibur instrument (BD Bioscience, Cambridge, UK).

Implantation of pMSCs into 3-D scaffolds

A hemostatic gelatin sponge, Spongostan^{TM} (Ferrosan Medical Device, MS0003, thickness 0.1 cm), was used as the 3D scaffold.(19) To perform transplantation, the scaffolds were cut into disks with a diameter of 0.8 cm, sterilized by 75% (v/v) ethanol and washed three times with phosphate-buffered saline. The sterile scaffold disks were then immersed in Opti-MEM medium (Gibco) before use. The sterile scaffold disks were individually placed onto the wells of a 48 well-plate. 5×10^4 cells/disk in 50 μL of medium were seeded throughout the surface of the scaffold disk and incubated for 3 hours to allow cell attachment before the addition of medium.

Cell distribution and morphology analysis after osteogenic differentiation

The above three groups then received 0.5 mL/well of osteogenic induction medium (OIM) to promote cell differentiation. The OIM medium was composed of complete MEM-α medium enriched with 10^{-7} M dexamethasone (Sigma), 10 mM β- glycerophosphate (Sigma) and 50 μg/mL ascorbic acid (Sigma).(19) The OIM medium was replenished every two or three days for a total of 7 days. The constructs in each time point were washed twice with phosphate buffered saline (PBS; GIBCO™, Invitrogen Corp., Carlsbad, CA) and fixed in 1.5% v/v glutaraldehyde in 0.14M sodium cacodylate (pH 7.4) for 30 mins at room temperature. Dehydration was performed by sequential immersion in serial diluted ethanol solutions of 50, 60, 70, 80, 90, and 100% v/v. The samples were then transferred to hexamethyldisilazane and air-dried at room temperature overnight. The cell distribution and morphology were analyzed by scanning electron microscopy (SEM) (Hitachi, SU8220).

Quantification of fluorescent in 3-D scaffolds

All samples were washed twice with PBS, fixed in 4% v/v formaldehyde (methanol-free; Polyscience) for 15 min, permeabilized with 0.1% v/v Triton X-100 for 5 minutes, and incubated in 10 mg/mL bovine serum albumin and 100 g/mL RNase for 45 minutes at room temperature. F-actin filaments were stained with Alexa Fluor-conjugated phalloidin (Molecular Probes) for 20 minutes, and nuclei were counterstained

with 10 g/mL propidium iodide (Sigma) for 10 minutes. Finally, the samples were washed with PBS and mounted in Vectashield®. Fluorescent images were recorded by confocal laser scanning microscopy (CLSM) (Leica, TCS SP8X). The quantitative distribution of fluorescent cells was analyzed with the same method illustrated in the monolayer section.

Osteogenic profiles in 3-D scaffolds

Alkaline phosphatase (ALP) staining and quantification

For staining on days 7 to 28, cells on the scaffold were washed twice with PBS and fixed for 5 min using 60% (v/v) citrate solution comprising 0.6 mL citrate concentrate solution (Sigma) in 29.4 mL deionized water and 20 mL acetone. The scaffolds were rinsed with deionized water and overnight stained with alkaline phosphatase staining solution. Alkaline phosphatase staining solution was a mixture of one part of naphthol AS-MX alkaline solution (Sigma) and 24 parts of fast violet stain solution (Sigma). On the next day, the staining solution was removed, and the scaffolds were washed five times with deionized water. Images of the stained discs were captured with a digital camera (Canon, PowerShot SX50 SH). The osteogenic quantification is assessed using an ALP assay kit (BioVision K412-500) after 7 to 28 days. The cells were washed with ice-cold PBS twice, and lysed using 300 µL RIPA (Radioimmunoprecipitation assay) lysis buffer (Sigma-Aldrich Corp., St Louis, MO, USA) for 5 min on ice. The cells were then rapidly scraped from the plate, and the cell lysates/RIPA buffer were transferred to a 1.5-mL microcentrifuge tube on ice for 20 min, followed by centrifugation at 8000 × g for 10 min at 4°C. The supernatant was then added to a new 1.5-mL microcentrifuge tube and stored at -20 °C., and then the volume was brought to 80 µL. Next, 50 µL of the 5 mM p-Nitrophenyl Phosphate (pNPP) solution was added to each well containing the test samples. The aliquots were incubated for 60 min at 25°C while protected from light. Subsequently, 20 µL of the stop solution was added to terminate the ALP activity in the sample. The absorbance at 405 nm was measured with a spectrophotometer (UV-Vis 8500). Then, the ALP activity was calculated using the following formula: [(Optical Density – Mean Optical Density of the Control Wells) × Total Volume × Dilution)/(18.45 × Sample Volume)].

Alizarin red S (ARS) staining and quantification

At days 7, 14, 21 and 28, cells cultured on the scaffolds were washed twice with PBS and fixed with 4% paraformaldehyde for 15 min. The fixative was removed and the discs with cells were rinsed with deionized water. The discs were stained with 2% ARS staining kit (Sigma-Aldrich Corp., St Louis, MO, USA) for 5 min to stain the calcium deposition on the discs. The staining solution was discarded, and the discs were carefully washed with deionized water until the excess stain was removed. The staining results were captured with a digital camera. To quantify the calcific stain on each scaffold disc, 1 mL/disc of 10 wt% cetylpyridinium chloride (Sigma-Aldrich Corp., St Louis, MO, USA) was added to the discs. The discs were left on an orbital shaker at 60 rpm for 1 h to completely resolve the dye from the discs. Finally, 100 µL of the dissolved solution from each disc was placed into a well of a 96-well plate and its absorbance measured at 540 nm with ELISA reader.

Immunohistochemistry (IHC) of osteogenic related markers

Histological slides of all three groups in different time points were incubated with citrate buffer (Dako, Glostrup, Denmark) at 60°C for heat-induced epitope retrieval and blocked with 1% hydrogen peroxide/methanol (Sigma-Aldrich, St Louis, MO, USA) for 30 min at room temperature. Subsequently, they were incubated overnight at 4°C with primary antibodies: collagen type I (Col-I) (1:1000, sc-59772, Santa Cruz Biotechnology, CA, USA) and osteocalcin (OC) (1:1000, sc-365797, Santa Cruz Biotechnology, CA, USA). The color reaction was developed with ready-to-use 3, 3'-diaminobenzidine (Dako Liquid DAB) color solution. The slides were counterstained with hematoxylin and visualized by a light microscope (Nikon Eclipse E600, Tokyo, Japan). The negative control used PBS instead of the primary antibody, and counterstaining was performed with hematoxylin.

Statistical analysis

All statistical analysis was performed using Student's t-test and two-way ANOVA. Analysis of variance (ANOVA) was performed by using GraphPad Prism 5 software. Differences with a p value of < 0.05 were considered statistically significant.

Results

Optimization of cell viability and transfection efficiency in group 2

In order to obtain optimal cell survival and transfection efficiency in group 2, the cells were transfected with either 1 µg or 2.5 µg of pEGFP, and in different concentration ratios of *Trans*IT®-2020: pEGFP-N1 of 1:1, 2:1, 3:1 and 4:1. Three days after transfection, we found that the concentration ratio of 4:1 was toxic to pMSCs (Figure 1). In the subsequent assessment of transfection efficiency, the 4:1 concentration was excluded. To evaluate transfection efficiency, the cells were treated with 1 µg of pEGFP-N1, and in different concentration ratios of *Trans*IT®-2020: pEGFP-N1 of 1:1, 2:1, and 3:1. The highest transfection efficiency, 50.6%, was achieved at a concentration ratio of 3:1 and using 1 µg pEGFP three days following transfection. The results were quantified and are represented by flow cytometry (Figure 2A). On fluorescent imaging, the 3:1 concentration ratio exhibited the most significant expression (Figure 2B), which is compatible with the flow cytometry data.

Monolayer culture

Fluorescent imaging and quantification after osteo-induction

The cell seeding density in all groups was 5 x 10^4 cells/well in 50 μL of medium on a 48 well-plate. The cells were seeded throughout the top side of the wells and then incubated for 3 hours to allow for cell attachment before adding the maintenance medium. Osteogenic induction medium was added starting on day 3. Using fluorescent microscopy, the expression of green fluorescence was observed from day 1 to day 28. Group 1 showed a greater number of cells than group 2, reflecting a greater proliferation capacity.

In group 1, highly proliferative and spindle-shaped eGFP-pMSCs were observed on day 1. Over the first week, cells were proliferative with a cuboidal shape. Proliferative activity waned from day 14 to day 28. In group 2, the transfected cells proliferated from the initial round shape to spindle-shaped in the first week. Green fluorescence decreased from day 14 to day 28, however, could still be observed. Only background fluorescence was observed in group 3 (Figure 3A). One day after seeding cells, no cell toxicity was observed by fluorescence microscopy. Quantitative fluorescence data from the images showed that expression of green fluorescence peaked on day 7, plateaued, then decreased after day 14 in both group 1 and group 2 (Figure 3B). There were no statistically significant differences between days 14, 21 and 28 in either group. The expression of green fluorescence in group 1 was higher than group 2 after the first two weeks. Minimal fluorescence was observed on day 7 in group 3. (Figure 3B).

Fluorescence evaluated by FACS after osteo-induction in monolayers

Flow cytometry was performed at different time points in all groups and revealed that the percentage of green fluorescent cells in group 1 and group 2 were 99.6% and 59.7% of total cell counts, respectively (Figure 3C). No green-fluorescent cells were observed in group 3 by FACS.

Co-existence of green fluorescence proteins and bone-like nodule

To evaluate the relation between eGFP and bone-like nodule formation after osteogenic differentiation, fluorescent and light microscopy images were merged for all groups. After osteogenic induction, bone-like nodules from differentiated cells were found on day 21 in all groups (Figure 4). A significantly greater number of mineralized bone-like nodules were formed between day 21 and day 28 in all groups. The green fluorescent signals were co-localized with nodules in group 1; however, a heterogeneous distribution of nodules without aggregated fluorescence was observed in group 2. No fluorescent cells were observed in the control groups (Figure 4).

In vitro 3-D culture

Cell distribution and morphology analysis

The increasing intensity of live cells from day 7 to 28 and observed polygonal morphology in all three groups indicated that the biocompatible scaffold(21) was suitable for pMSCs attachment and proliferation (Figure 5A). SEM showed that the connected pores were almost entirely covered by MSC proliferation on day 21 in group 1 and on day 28 in groups 2 and 3. The calcified nodule in all three groups gradually increased from day 14 to day 28 (Figure 5A).

Fluorescence imaging and quantification after osteogenic differentiation

CLSM was performed to characterize the *in vitro* distribution of pMSCs in the scaffolds. The green fluorescence distribution can be observed on the surface view from day 7 to day 28 in both group 1 and group 2. Significantly higher eGFP expression was observed at each subsequent time point in group 1, and with greater abundance than in group 2. No fluorescent cells were observed in group 3 (Figure 5B).

Fluorescence quantification showed that the expression in group 1 was significantly higher than in group 2 at each time point. (Figure 5C). The level of eGFP expression on days 21 and 28 were significantly higher than days 7 and 14 in group 1. In group 2, expression on day 21 was significantly higher than day 7 (Figure 5D). Only background fluorescence was observed in group 3 (Figure 5C, 5D).

Staining and activity of osteogenic profiles

Alkaline phosphatase

Light microscopy for alkaline phosphatase staining on the scaffolds showed slightly positive staining on day 7 and increasing staining intensity on days 14, 21 and 28 in all three groups (Figure 6A). ALP activity showed significantly increasing value from day 7 to day 21 and day 28 in all groups (Figure 6B). There was no statistically significant difference in ALP activity between group 1 and group 3 for the duration of the osteogenesis period. Activity was higher in group 1 compared to group 2 on days 14 and 28 (Figure 6C).

Alizarin red staining

ARS, an indicator of bone mineralization, was negative on day 14 in all groups (Figure 7A). On day 21 in group 1 and group 3, and on day 28 in group 2, there was positive staining with a deep red color to indicate bone nodule formation.

The ARS quantification assay was performed at different time points, and the absorbance was measured at 540 nm using an ELISA reader. The absorbance value significantly increased from day 14 to day 21 in all three groups. On day 28, calcium deposition was significantly lower in group 2 compared to group 1 ($p < 0.05$). This value was also significantly lower in group 2 compared to group 3 on day 14 (Figure 7B).

Immunohistochemistry of osteogenic related markers

Immunohistochemistry was conducted using Col-I and OC as markers to evaluate bone formation (Figure 8). Col-I was highly expressed on day 28 in group 1 and 3 compared to group 2, implying that there were significantly higher rates of osteogenesis in groups 1 and 3. Expression of Col-I was detected on day 14 because the scaffold, itself, is highly composed of collagen (Figure 8A).

Immunohistochemistry for OC demonstrated significant expression on day 21 in all three groups. On day 28, expression was significantly higher in groups 1 and 3 than in group 2 (Figure 8B).

Discussion

The incorporation of a stably expressed eGFP into the genome of MSCs, with whole differentiated progenies, provides a tool to trace their presence, migration, and formation of tissues after transplantation. Stem cells possess two key abilities: 1) differentiation and 2) self-renewal. In turn, fluorescent dyes such as PPKH26, or Hoechst 33342 cannot be used, considering their tracking ability is

limited to the parent cell after division(22)(23). Establishing a stable and effectively traced stem cell line, to follow its products and the migration of transplanted stem cells, is critical in tissue engineering. Enhanced green fluorescent proteins in transgenic animals and non-virally transfected MSCs are commonly used to trace differentiated products, but have yet to be compared.

Cells in group 1 comprised CAG hybrid promoter-driven eGFP-MSCs derived from the transgenic pigs, which were made from plasmid-microinjected fertilized eggs. These have been proven to exhibit homogeneous surface epitopes and possess classic trilineage differentiation potential into osteogenic, adipogenic, and chondrogenic lineages, and with maintenance of robust eGFP expression in all differentiated progeny(10). Increasing green fluorescence was observed from day 3 to day 28 after cells were seeded to the scaffolds, and following transplantation to the pig's calvarial defect(19).

Genetically modifying cells using transfection reagents has increasingly become a popular alternative to viral transfection, because of its reduced potential for viral infection and tumorigenesis(24)(25). TransIT-2020 (Mirus, Madison, WI, USA), among six cationic and lipid polymers for bone marrow-derived stromal cells(14), showed the highest GFP expression without decreasing cell recovery; this technique has been widely applied with *in vivo* studies.(26)(18)

In the study, there are two reasons why we chose to use a transgenic pig model instead of rat model. First, the bone regeneration rate was found to be similar between pigs (1.2 -1.5 mm per day) and humans (1.0 - 1.5 mm per day).(15)(27)(19) Second, several test groups could be performed in a same large animal like pig, which can potentially eliminate individual bias and increase the validity of experimental data.(19)

To obtain the highest cell survival rate in the non-virally transfected group, cells were transfected with different concentration ratios of TransIT®-2020 and plasmid eGFP (Figure 1). The transfection efficiency and viability of pMSCs were 50.6% and over 96%, respectively, at a 3:1 concentration ratio and 1 μg of eGFP plasmid introduced in the following osteogenic induction experiments (Figure 2). Cheung WY, et al. transfected GFP to human bone marrow-derived mesenchymal stem cells using a 3:1 concentration of TransIT-2020: plasmid and yielded 24–36% GFP-expressing cells with a viability of 85–96%.(14) In this study, we also used a 3:1 concentration of TransIT-2020: plasmid, however, we yielded 50.6% GFP-expressing cells and 96-98% viability. This difference may be higher than their study in consideration of the difference in cell density per plasmid and animal species.(28)(29) A higher transfection rate, via viral or non-viral methods, was demonstrated in porcine cells compared to bovine cells, even when controlling for the same culture environment and passage number.(30)

The fluorescent images after osteogenic differentiation in the monolayer culture were significantly different between groups. Group 1 was characterized by highly proliferative and spindle-shaped eGFP-MSCs, which were observed on day 1 and increased throughout the first week; signals decreased from day 14 to day 28. In group 2, the transfected cells extended in spindle-shaped formations starting on day 7 instead of day 1. Green color decreased from day 14 to day 28, but could still be observed on day 28. The quantification data showed that the expression of eGFP peaked on day 7, significantly decreased on

day 14, and remained consistent to day 28 in both groups. Higher expression was observed in group 1 than in group 2 on day 1 and day 7, but no difference was observed after day 14. Flow cytometry revealed that the percentages of eGFP cells in groups 1 and 2 were 99.6% and 59.7% of total cell counts, respectively, at almost every time point. The different quantification results between imaging and flow cytometry techniques may be due to differentiated cells attaching to the plate, thus preventing them from being suspended in the buffer while performing flow cytometry. The cells in the suspension should be undifferentiated, and the fluorescent percentage is similar to the transfection data in Figure 2. The implication of this finding is that successfully transfected cells in group 2 maintained stable transfection potential even when cultured for 28 days.

To evaluate the relationship between eGFP signal and bone-like nodule formation after induction, fluorescence and light microscopy images were merged for all groups. The final products demonstrated bone-like nodule formation in the monolayer culture for 21 days following osteogenic induction (Figure 4). The green-fluorescent signal was co-localized with the bone-like nodule in group 1, however we observed a heterogeneous distribution of eGFP without clear aggregation around nodules in group 2. The different aggregation patterns in group 1 and group 2 can be attributed to two reasons. First, by flow cytometry, the percentage of free eGFP cells was over 99% in group 1, but only 60% in group 2. Significantly more aggregates would be expected if a higher number of non-adherent cells were present in the initial solution. Second, migration and recruitment of MSCs were observed during nodule formation. Factors like SDF-1, BMPs, TGFβ-1 have been shown to be involved in MSCs migration during bone formation.(31)(32)(33)(34) On fluorescence imaging, highly proliferative and spindle-shaped cells were detected earlier in group 1 than in group 2, These findings suggest that more bone-like nodules would be expected in group 1, and in turn, larger MSC recruitment and aggregation.

Consistent with data from SEM imaging, modified intensity density of green fluorescence in the 3-D scaffolds increased from day 14 in both group 1 and group 2. Moreover, the MSCs showed extension of their filopodia into the highly porous, biocompatible scaffolds(21). Two-dimensional space limitations, extracellular environments, cell morphologies, and division methods each contribute to MSC growth restriction in a monolayer culture(35)(36). Together, these factors explain the decline in green fluorescence expression after day 14, compared to the robust proliferation observed in 3-D culture.

At each week, green fluorescence expression was significantly higher in group 1 than in group 2, likely because the images were captured from the surfaces of scaffolds; thus, the cells inside the gel foam could not be visualized. Additional factors including growth tropism and differing cell percentages may have also contributed to the variances in proliferation between the limited 2-D environment and the disseminated 3-D scaffolds.(37,38)

Understanding the osteogenic potential of pMSCs after eGFP plasmid transfection is crucial in tissue engineering. Three weeks after osteoinducing the scaffold-seeded cells, mineralized nodules with osteoid matrix were observed in larger quantities in group 1 than group 2. This observation was confirmed by quantifying their respective osteogenic profiles (Figures 7C and 8B). On day 28, IHC staining for OC and

COL-I markers revealed higher expression in groups 1 and 3 than group 2. The osteogenic quantification data for group 1 and group 3 were similar, likely because MSCs from eGFP-transgenic pigs have been shown to keep their unique polygonal morphology and differentiation capability, in contrast to MSCs from non-transgenic pigs.(39)(29)(40)(41) In our study, we demonstrated high cell viability and high transfection efficiency in our eGFP-transfected pMSCs. One interpretation is that the transfection reagent was not particularly toxic to the cells, such that changes in differentiation potential would influence our results. Non-viral gene delivery using cationic lipids such as *Trans*IT®-2020 has been shown to be non-toxic in a selected range of concentrations for transfection. In our study, we observed a 99% cell survival rate using the 3:1 concentration ratio, however, this does not imply that all surviving cells were healthy. The cationic lipid reagent conjugated to the plasmid, when transferred into the cell nucleus, has the potential for charge-charge interactions and changes in surface receptor binding affinities that may interfere with normal cellular function(42)(43).

Evidence has shown that the transfection efficiency and survival rate of MSCs can change, depending on the tissue source, passage numbers, and individual donors.(44) We controlled for individual and tissue differences in groups 2 and 3 by using cells from the same pig and from the same donor site. Differences in passage number, however, were not controlled. Mesenchymal stem cells universally express surface markers such as CD73+, CD90+, and CD105+. Cell-specific surface markers can vary considerably between tissues or donors, resulting in different proliferative capacities, differentiation potentials, and immunomodulatory potencies (45)(46)(47), which may explain the differences in osteogenesis between groups 1 and 2. In past studies regarding transgene microinjected embryos, the literature reported success rates below 10% for ultimately developing into transgenic pigs(48)(49), suggesting that *in vitro*-fertilized pig zygotes with low survival or poor differential potential were eliminated before birth. In essence, the differentiation and self-renewal capabilities of MSCs derived from mature transgenic pigs were assured through natural selection.

Conclusions

Stable transfection was observed in MSCs derived from both the transgenic pig model and the non-viral transfection method. Green fluorescent protein expression is limited in monolayer culture compared to 3-D culture, due to limitations on the available space for cell proliferation. Osteogenesis in cells derived from transgenic pigs or non-transfected cells was superior to *Trans*IT®-2020 transfected pMSCs, likely owing to toxic intra- and extracellular membrane changes. Long-term *in vivo* studies comparing MSCs derived from transgenic pigs and MSCs treated with transfection reagents would provide support to these findings.

Abbreviations

pMSCs pig mesenchymal stem cells

eGFP enhanced green fluorescent protein

FBS fetal bovine serum

PBS phosphate- buffered saline

MEM minimum essential medium

pEGFP-N1 plasmid enhanced green fluorescent protein gene

FACS fluorescence-activated cell sorting

OIM osteogenic induction medium

Modified IntDen modified integrated density

SEM scanning electron microscopy

CLSM confocal laser scanning microscopy

ALP Alkaline phosphatase

RIPA Radioimmunoprecipitation assay

pNPP p-Nitrophenyl Phosphate

ARS Alizarin red S

Col-I collagen type I

OC osteocalcin OC

IHC Immunohistochemistry

ANOVA Analysis of variance

Declarations

Ethics approval and consent to participate

This study was carried out in strict accordance to the Guide for the Care and Use of Laboratory Animals of the National Institutes of Health. All animal cells were retrieved under the approved animal protocols by the Institutional Animal Care and Use Committee of National Taiwan University (NTU107-EL-00128).

Consent for publication

Not applicable

Availability of data and materials

The data that support the findings of this study are available on request from the corresponding author.

Competing interests

The authors declare that they have no competing interests.

Funding

This work was supported by the Chang Gung Memorial Hospital (grant No. CMRPG3G2061) and the Ministry of Science and Technology, Taiwan, R.O.C. (grant No. MOST 108-2313-B-002-014-).

Author's contributions:

Ming-Kai Hsieh: Conception and design, data analysis and interpretation, manuscript writing

Chia-Jung Wu: Provision of study material, collection and assembly of data

Chi-Yun Wang: Provision of study material or patients, data analysis and interpretation

Tsung-Ting Tsai: Administrative support, manuscript writing

Chi-Chien Niu: Administrative support

Po-Liang Lai: Conception and design, data analysis and interpretation,

Shinn-Chih Wu: Financial support, final approval of manuscript

All authors read and approved the final manuscript.

Acknowledgments

We would like to thank the Microscope Core Laboratory at the Center for Advanced Molecular Imaging and Translation and the Laboratory Animal Center of Linkou Chang Gung Memorial Hospital.

References

1. SquillaroT, PelusoG, GalderisiU. Clinical trials with mesenchymal stem cells: An update. Vol. 25, Cell Transplantation. Cognizant Communication Corporation; 2016. p. 829–48.
2. KodeJA, MukherjeeS, JoglekarMV, HardikarAA. Mesenchymal stem cells: immunobiology and role in immunomodulation and tissue regeneration. Cytotherapy [Internet]. 2009 [cited 2020 Jan 4];11(4):377–91. Available from: http://www.ncbi.nlm.nih.gov/pubmed/19568970
3. HuiJHP, LiL, TeoY-H, OuyangH-W, LeeE-H. Comparative study of the ability of mesenchymal stem cells derived from bone marrow, periosteum, and adipose tissue in treatment of partial growth arrest

in rabbit. Tissue Eng [Internet]. [cited 2020 Jan 4];11(5–6):904–12. Available from: http://www.ncbi.nlm.nih.gov/pubmed/15998230

4. ChalfieM. GREEN FLUORESCENT PROTEIN. Photochem Photobiol. 1995;62(4):651–6.
5. ChalfieM, TuY, EuskirchenG, WardWW, PrasherDC. Green fluorescent protein as a marker for gene expression. Science (80-). 1994;263(5148):802–5.
6. KandelES, ChangBD, SchottB, ShtilAA, GudkovAV, RoninsonIB. Applications of green fluorescent protein as a marker of retroviral vectors. Somat Cell Mol Genet [Internet]. 1997 Sep [cited 2020 Jan 4];23(5):325–40. Available from: http://www.ncbi.nlm.nih.gov/pubmed/9546076
7. BainbridgeJW, StephensC, ParsleyK, DemaisonC, HalfyardA, ThrasherAJ, et al. In vivo gene transfer to the mouse eye using an HIV-based lentiviral vector; efficient long-term transduction of corneal endothelium and retinal pigment epithelium. Gene Ther [Internet]. 2001 Nov [cited 2020 Jan 4];8(21):1665–8. Available from: http://www.ncbi.nlm.nih.gov/pubmed/11895005
8. Stable and efficient gene transfer into the retina using an HIV-based - PubMed - NCBI [Internet]. [cited 2020 Jan 4]. Available from: https://www.ncbi.nlm.nih.gov/pubmed/?term=Stable+and+efficient+gene+transfer+into+the+retina+using+an+HIV-based+lentiviral+vector.
9. Mutation-Based Therapeutic Strategies for Duchenne Muscular Dystrophy: From Genetic Diagnosis to Therapy. - PubMed - NCBI [Internet]. [cited 2020 Jan 4]. Available from: https://www.ncbi.nlm.nih.gov/pubmed/30836656
10. HsiaoFSH, LianWS, LinSP, LinCJ, LinYS, ChengECH, et al. Toward an ideal animal model to trace donor cell fates after stem cell therapy: production of stably labeled multipotent mesenchymal stem cells from bone marrow of transgenic pigs harboring enhanced green fluorescence protein gene. J Anim Sci [Internet]. 2011 Nov [cited 2020 Jan 4];89(11):3460–72. Available from: http://www.ncbi.nlm.nih.gov/pubmed/21705633
11. KemterE, CohrsCM, SchäferM, SchusterM, SteinmeyerK, Wolf-van BuerckL, et al. INS-eGFP transgenic pigs: a novel reporter system for studying maturation, growth and vascularisation of neonatal islet-like cell clusters [Internet]. Vol. 60, Diabetologia. Springer Verlag; 2017 [cited 2020 Feb 16]. p. 1152–6. Available from: http://www.ncbi.nlm.nih.gov/pubmed/28315950
12. KuromeM, LeuchsS, KesslerB, KemterE, JemillerEM, FoersterB, et al. Direct introduction of gene constructs into the pronucleus-like structure of cloned embryos: a new strategy for the generation of genetically modified pigs. Transgenic Res [Internet]. 2017 Apr 1 [cited 2020 Feb 18];26(2):309–18. Available from: http://www.ncbi.nlm.nih.gov/pubmed/27943082
13. ElslerS, SchettingS, SchmittG, KohnD, MadryH, CucchiariniM. Effective, safe nonviral gene transfer to preserve the chondrogenic differentiation potential of human mesenchymal stem cells. J Gene Med [Internet]. 2012 Jul [cited 2020 Jan 4];14(7):501–11. Available from: http://www.ncbi.nlm.nih.gov/pubmed/22711470
14. CheungWY, HoveyO, GobinJM, MuradiaG, MehicJ, WestwoodC, et al. Efficient Nonviral Transfection of Human Bone Marrow Mesenchymal Stromal Cells Shown Using Placental Growth Factor

Overexpression. Stem Cells Int [Internet]. 2018 [cited 2020 Jan 13];2018:1310904. Available from: http://www.ncbi.nlm.nih.gov/pubmed/30675166

15. DomenighettiAA, ChuP-H, WuT, SheikhF, GokhinDS, GuoLT, et al. Loss of FHL1 induces an age-dependent skeletal muscle myopathy associated with myofibrillar and intermyofibrillar disorganization in mice. Hum Mol Genet [Internet]. 2014 Jan 1 [cited 2020 Jan 4];23(1):209–25. Available from: http://www.ncbi.nlm.nih.gov/pubmed/23975679
16. ShitomiY, ThøgersenIB, ItoN, LeitingerB, EnghildJJ, ItohY. ADAM10 controls collagen signaling and cell migration on collagen by shedding the ectodomain of discoidin domain receptor 1 (DDR1). Mol Biol Cell [Internet]. 2015 Feb 15 [cited 2020 Jan 4];26(4):659–73. Available from: http://www.ncbi.nlm.nih.gov/pubmed/25540428
17. ChongYC, MannRK, ZhaoC, KatoM, BeachyPA. Bifurcating action of Smoothened in Hedgehog signaling is mediated by Dlg5. Genes Dev [Internet]. 2015 Feb 1 [cited 2020 Jan 4];29(3):262–76. Available from: http://www.ncbi.nlm.nih.gov/pubmed/25644602
18. HsiehM-K, WuC-J, ChenC-C, TsaiT-T, NiuC-C, WuS-C, et al. BMP-2 gene transfection of bone marrow stromal cells to induce osteoblastic differentiation in a rat calvarial defect model. Mater Sci Eng C. 2018;91.
19. HsiehM-K, WuC-J, SuX-C, ChenY-C, TsaiT-T, NiuC-C, et al. Bone regeneration in Ds-Red pig calvarial defect using allogenic transplantation of EGFP-pMSCs - A comparison of host cells and seeding cells in the scaffold. PLoS One [Internet]. 2019 [cited 2020 Jan 3];14(7):e0215499. Available from: http://www.ncbi.nlm.nih.gov/pubmed/31318872
20. JensenJ, TvedesøeC, RölfingJHD, FoldagerCB, LysdahlH, KraftDCE, et al. Dental pulp-derived stromal cells exhibit a higher osteogenic potency than bone marrow-derived stromal cells in vitro and in a porcine critical-size bone defect model. SICOT-J [Internet]. 2016 Apr 20 [cited 2020 Jan 4];2:16. Available from: http://www.ncbi.nlm.nih.gov/pubmed/27163105
21. KuoZ-K, LaiP-L, TohEK-W, WengC-H, TsengH-W, ChangP-Z, et al. Osteogenic differentiation of preosteoblasts on a hemostatic gelatin sponge. Sci Rep [Internet]. 2016 [cited 2020 Jan 15];6:32884. Available from: http://www.ncbi.nlm.nih.gov/pubmed/27616161
22. RieckB, SchlaakS. In vivo tracking of rat preadipocytes after autologous transplantation. Ann Plast Surg [Internet]. 2003 Sep [cited 2020 Jan 17];51(3):294–300. Available from: http://www.ncbi.nlm.nih.gov/pubmed/12966243
23. MohorkoN, Kregar-VelikonjaN, RepovsG, GorensekM, BresjanacM. An in vitro study of Hoechst 33342 redistribution and its effects on cell viability. Hum Exp Toxicol [Internet]. 2005 Nov [cited 2020 Jan 17];24(11):573–80. Available from: http://www.ncbi.nlm.nih.gov/pubmed/16323574
24. GiaccaM, ZacchignaS. Virus-mediated gene delivery for human gene therapy. Vol. 161, Journal of Controlled Release. 2012. p. 377–88.
25. GuptaV, Linn CadieuxC, McMenaminD, Angelica Medina-JaszekC, ArifM, AhonkhaiO, et al. Adeno-associated virus-mediated expression of human butyrylcholinesterase to treat organophosphate poisoning. PLoS One. 2019;14(11).

26. TomizawaM, ShinozakiF, MotoyoshiY, SugiyamaT, YamamotoS, SueishiM. Dual gene expression in embryoid bodies derived from human induced pluripotent stem cells using episomal vectors. Tissue Eng - Part A. 2014 Dec 1;20(23–24):3154–62.
27. SchlegelKA, LangFJ, DonathK, KulowJT, WiltfangJ. The monocortical critical size bone defect as an alternative experimental model in testing bone substitute materials. Oral Surg Oral Med Oral Pathol Oral Radiol Endod [Internet]. 2006 Jul [cited 2020 Jan 13];102(1):7–13. Available from: http://www.ncbi.nlm.nih.gov/pubmed/16831666
28. KallaD, KindA, SchniekeA. Genetically Engineered Pigs to Study Cancer. Int J Mol Sci [Internet]. 2020 Jan 13 [cited 2020 Jan 17];21(2):488. Available from: https://www.mdpi.com/1422-0067/21/2/488
29. PerlebergC, KindA, SchniekeA. Genetically engineered pigs as models for human disease. Vol. 11, DMM Disease Models and Mechanisms. Company of Biologists Ltd; 2018.
30. ColleoniS, DonofrioG, LagutinaI, DuchiR, GalliC, LazzariG. Establishment, differentiation, electroporation, viral transduction, and nuclear transfer of bovine and porcine mesenchymal stem cells. Cloning Stem Cells [Internet]. 2005 [cited 2020 Jan 24];7(3):154–66. Available from: http://www.ncbi.nlm.nih.gov/pubmed/16176125
31. SuP, TianY, YangC, MaX, WangX, PeiJ, et al. Mesenchymal stem cell migration during bone formation and bone diseases therapy. Vol. 19, International Journal of Molecular Sciences. MDPI AG; 2018.
32. KitaoriT, ItoH, SchwarzEM, TsutsumiR, YoshitomiH, OishiS, et al. Stromal cell-derived factor 1/CXCR4 signaling is critical for the recruitment of mesenchymal stem cells to the fracture site during skeletal repair in a mouse model. Arthritis Rheum. 2009 Mar;60(3):813–23.
33. NgJ, WeiY, ZhouB, BurapachaisriA, GuoE, Vunjak-NovakovicG. Extracellular matrix components and culture regimen selectively regulate cartilage formation by self-assembling human mesenchymal stem cells in vitro and in vivo. Stem Cell Res Ther [Internet]. 2016 [cited 2020 Jan 21];7(1):183. Available from: http://www.ncbi.nlm.nih.gov/pubmed/27931263
34. MassaguéJ, SeoaneJ, WottonD. Smad transcription factors. Vol. 19, Genes and Development. 2005. p. 2783–810.
35. SokolovaV, Rojas-SánchezL, BiałasN, SchulzeN, EppleM. Calcium phosphate nanoparticle-mediated transfection in 2D and 3D mono- and co-culture cell models. Acta Biomater. 2019 Jan 15;84:391–401.
36. KapałczyńskaM, KolendaT, PrzybyłaW, ZajączkowskaM, TeresiakA, FilasV, et al. 2D and 3D cell cultures – a comparison of different types of cancer cell cultures. Arch Med Sci. 2018;14(4):910–9.
37. KosticA, LynchCD, SheetzMP. Differential matrix rigidity response in breast cancer cell lines correlates with the tissue tropism. PLoS One [Internet]. 2009 Jul 23 [cited 2020 Jan 29];4(7):e6361. Available from: http://www.ncbi.nlm.nih.gov/pubmed/19626122
38. LiR, HebertJD, LeeTA, XingH, Boussommier-CallejaA, HynesRO, et al. Macrophage-Secreted TNFα and TGFβ1 Influence Migration Speed and Persistence of Cancer Cells in 3D Tissue Culture via Independent Pathways. Cancer Res [Internet]. 2017 [cited 2020 Jan 29];77(2):279–90. Available from: http://www.ncbi.nlm.nih.gov/pubmed/27872091

39. KallaD, KindA, SchniekeA. Genetically Engineered Pigs to Study Cancer. Int J Mol Sci [Internet]. 2020 Jan 13 [cited 2020 Jan 20];21(2):488. Available from: https://www.mdpi.com/1422-0067/21/2/488
40. SmatlikovaP, JuhasS, JuhasovaJ, SuchyT, Hubalek KalbacovaM, ElledérovaZ, et al. Adipogenic Differentiation of Bone Marrow-Derived Mesenchymal Stem Cells in Pig Transgenic Model Expressing Human Mutant Huntingtin. J Huntingtons Dis [Internet]. 2019 [cited 2020 Jan 20];8(1):33–51. Available from: http://www.ncbi.nlm.nih.gov/pubmed/30584151
41. ShangP, WangZ, ChambaY, ZhangB, ZhangH, WuC. A comparison of prenatal muscle transcriptome and proteome profiles between pigs with divergent growth phenotypes. J Cell Biochem [Internet]. 2019 Apr [cited 2020 Jan 20];120(4):5277–86. Available from: http://www.ncbi.nlm.nih.gov/pubmed/30302803
42. HamannA, NguyenA, PannierAK. Nucleic acid delivery to mesenchymal stem cells: a review of nonviral methods and applications. J Biol Eng [Internet]. 2019 [cited 2020 Jan 21];13:7. Available from: http://www.ncbi.nlm.nih.gov/pubmed/30675180
43. XiangS, TongH, ShiQ, FernandesJC, JinT, DaiK, et al. Uptake mechanisms of non-viral gene delivery. Vol. 158, Journal of Controlled Release. 2012. p. 371–8.
44. ReiserA, WoschéeD, MehrotraN, KrzysztońR, StreyHH, RädlerJO. Correlation of mRNA delivery timing and protein expression in lipid-based transfection. Integr Biol (Camb). 2019 Dec 31;11(9):362–71.
45. KetterlN, BrachtlG, SchuhC, BiebackK, SchallmoserK, ReinischA, et al. A robust potency assay highlights significant donor variation of human mesenchymal stem/progenitor cell immune modulatory capacity and extended radio-resistance. Stem Cell Res Ther [Internet]. 2015 Dec 1 [cited 2020 Jan 21];6:236. Available from: http://www.ncbi.nlm.nih.gov/pubmed/26620155
46. deWolfC, van deBovenkampM, HoefnagelM. Regulatory perspective on in vitro potency assays for human mesenchymal stromal cells used in immunotherapy. Vol. 19, Cytotherapy. Elsevier B.V.; 2017. p. 784–97.
47. QadanMA, PiuzziNS, BoehmC, BovaW, MoosM, MiduraRJ, et al. Variation in primary and culture-expanded cells derived from connective tissue progenitors in human bone marrow space, bone trabecular surface and adipose tissue. Cytotherapy [Internet]. 2018 [cited 2020 Jan 21];20(3):343–60. Available from: http://www.ncbi.nlm.nih.gov/pubmed/29396254
48. UchidaM, ShimatsuY, OnoeK, MatsuyamaN, NikiR, IkedaJE, et al. Production of transgenic miniature pigs by pronuclear microinjection. Transgenic Res. 2001;10(6):577–82.
49. LiZ, ZengF, MengF, XuZ, ZhangX, HuangX, et al. Generation of transgenic pigs by cytoplasmic injection of piggyBac transposase-based pmGENIE-3 plasmids. Biol Reprod [Internet]. 2014 May [cited 2020 Jan 20];90(5):93. Available from: http://www.ncbi.nlm.nih.gov/pubmed/24671876

Figures

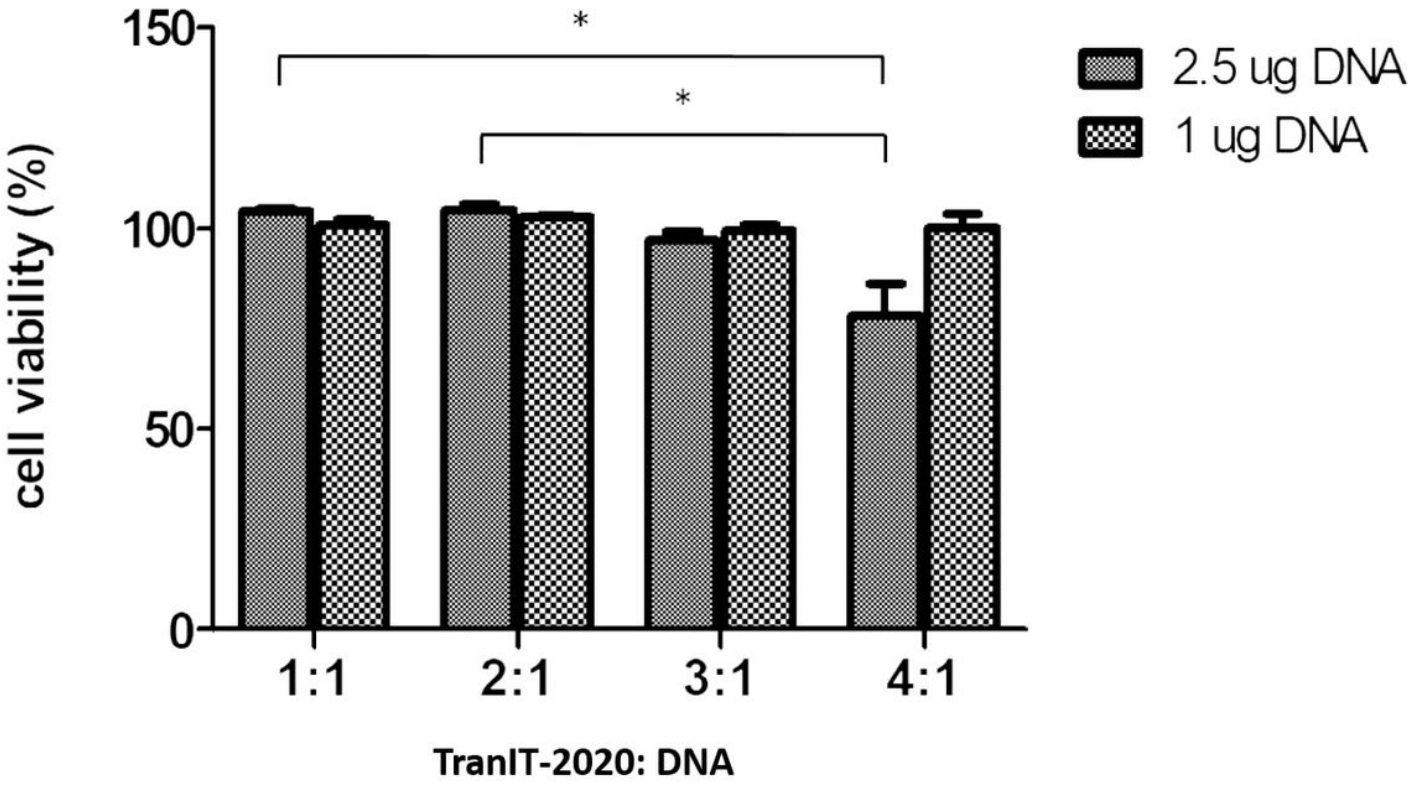

Figure 1

Optimization of cell viability in group 2 The pMSCs were transfected with either 1 µg, or 2.5 µg of pEGFP in different concentration ratios of TransIT®-2020: pEGFP of 1:1, 2:1, 3:1 and 4:1. Three days after transfection, we found that the 4:1 concentration ratio is toxic to pBMSCs, where cell viability decreased to 77.3 %.

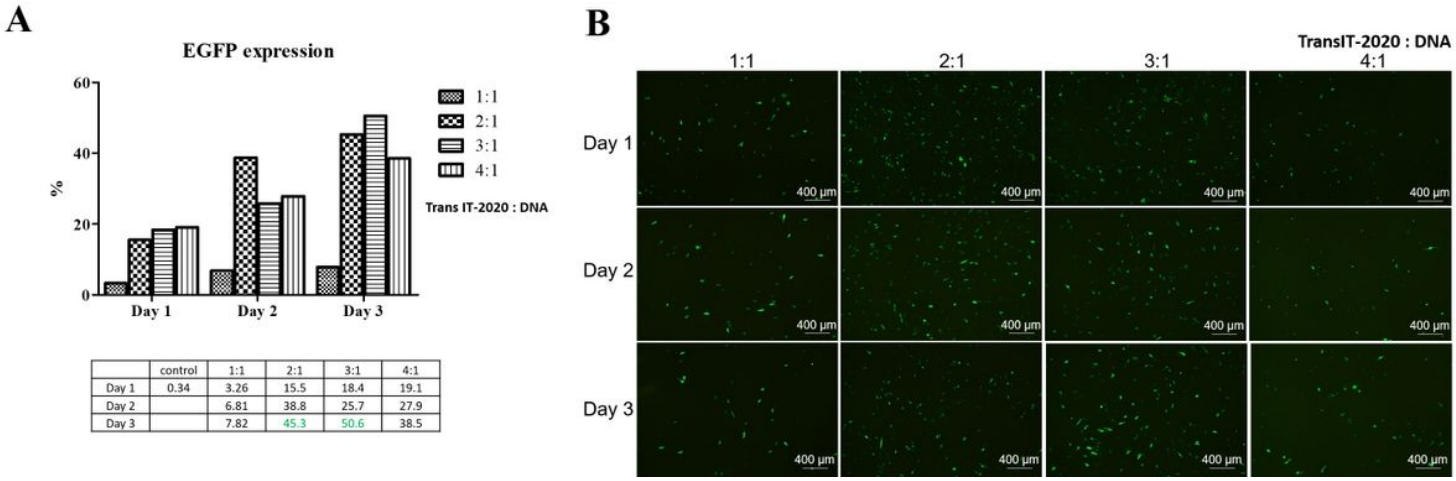

	control	1:1	2:1	3:1	4:1
Day 1	0.34	3.26	15.5	18.4	19.1
Day 2		6.81	38.8	25.7	27.9
Day 3		7.82	45.3	50.6	38.5

Figure 2

Optimization of transfection efficiency in group 2 The pMSCs were treated with 1µg of pEGFP-N1 and different ratios of TransIT®-2020: pEGFP-N1 of 1:1, 2:1, and 3:1. Transfection efficiency peaked at 50.6%

using a concentration ratio of 3:1 with 1 μg pEGFP 3 days after transfection, and are quantified as flow cytometry data (Figure 2A). On fluorescent imaging, the 3:1 concentration ratio had the highest transfection performance compared to other ratios, consistent with the flow cytometry data (Figure 2B).

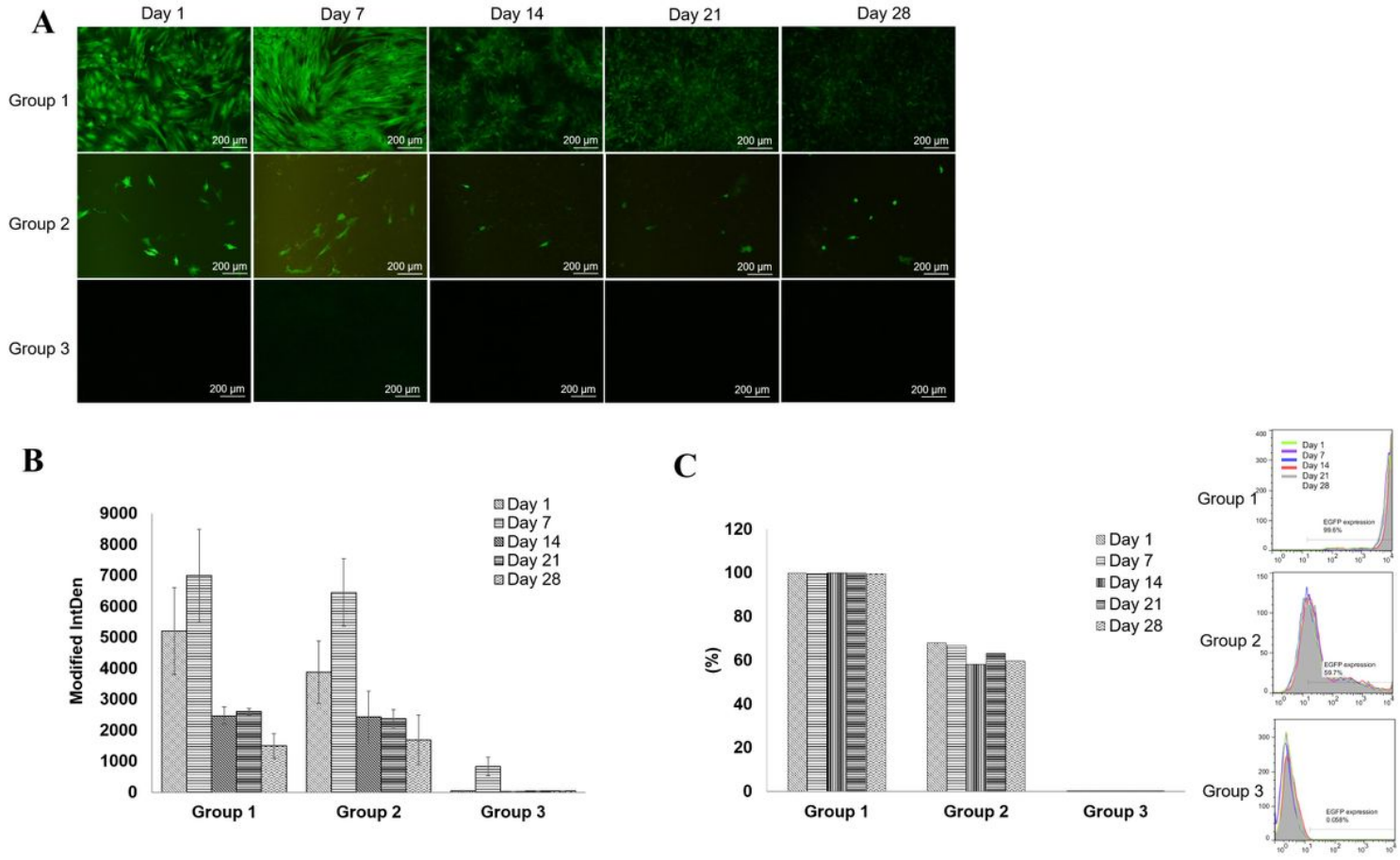

Figure 3

Fluorescence evaluation after osteoinduction in monolayer culture. Green fluorescence from day 1 to day 28 was observed by fluorescent microscopy after osteogenic induction in the monolayer culture (Figure 3A). Highly proliferative and spindle-shaped eGFP-pMSCs was observed starting day 1 in group 1 and day 7 in group 2, and no fluorescence was observed in group 3. The eGFP quantification data from imaging showed that expression peaked on day 7 but decreased after day 14 in both group 1 and 2 (Figure 3B). Flow cytometry showed that the percentage of green fluorescent cells in group 1 and 2 were 99.6% and 59.7% of total cell counts, respectively (Figure 3C).

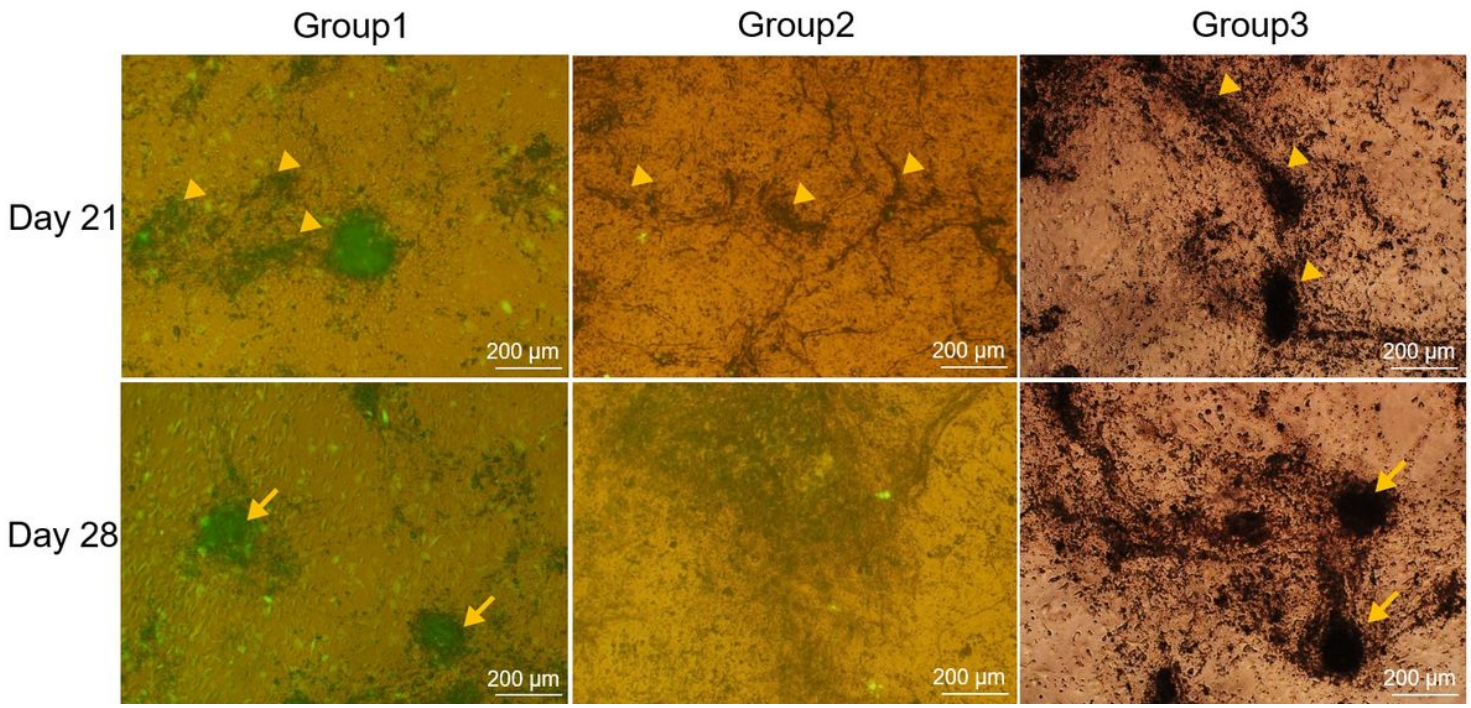

Figure 4

Co-existence of green fluorescence proteins and bone-like nodules. Merged pictures from fluorescent and light microscopy showed bone-like nodules forming from differentiated cells on day 21 after osteogenic induction. In all groups, a larger quantity of mineralized bone-like nodules was formed on day 28 compared to day 21. Aggregations of eGFP cells were uniquely observed in group 1.

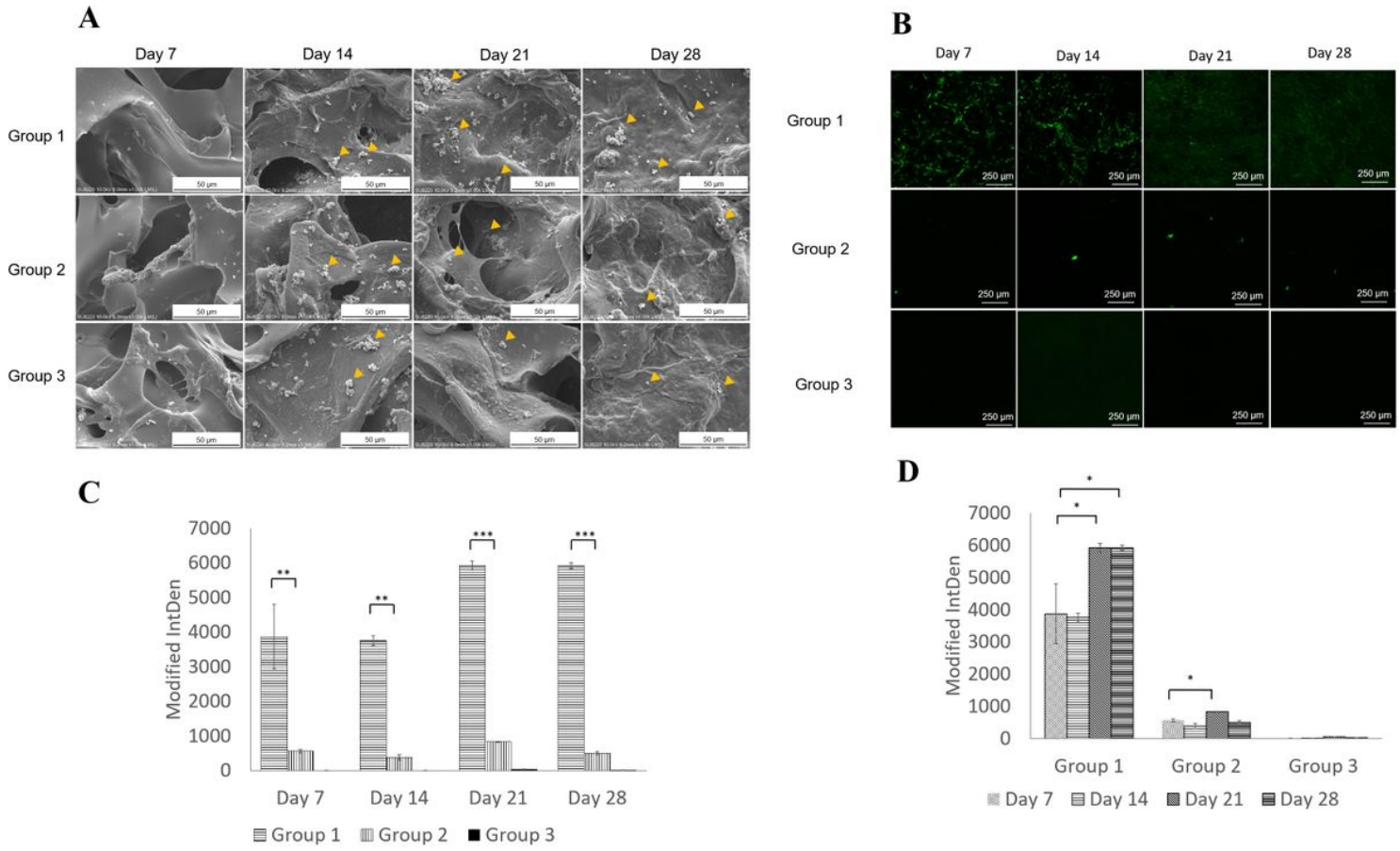

Figure 5

Morphology analysis and Fluorescence evaluation after osteogenic induction in 3-D scaffold Exhibition of polygonal cell morphology and increasing signal intensity was observed from day 7 to 28 in all three groups. Scanning electron microscopy showed that the calcified nodule gradually increased in size from day 14 to day 28 in all three groups (Figure 5A). On confocal laser scanning microscopy, green fluorescence was observed on the scaffolds from day 7 to day 28 in groups 1 and 2. Significantly higher eGFP expression was observed at each time point in groups 1 and 2 (Figure 5B). Quantification showed that the expression in group 1 was significantly higher than group 2 at each time point (Figure 5C). EGFP expression on days 21 and 28 was significantly higher than days 7 and 14 in group; in group 2, expression on day 21 was significantly higher than day 7 (Figure 5D).

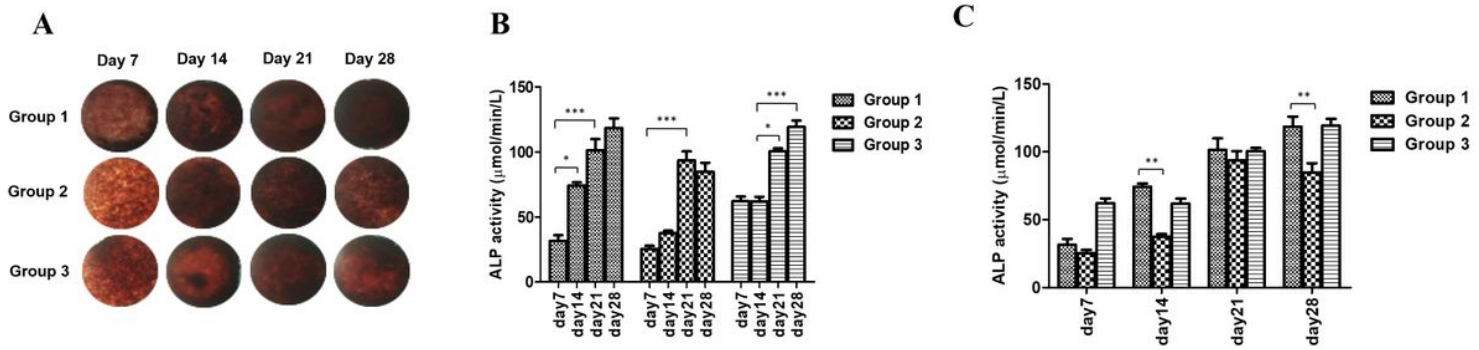

Figure 6

Alkaline phosphatase staining and activity Alkaline phosphatase (ALP) staining of the scaffolds was visualized on day 7, and increased in intensity on days 14, 21, and 28 in all three groups (Figure 6A). Alkaline phosphatase activity significant increased from day 7 to day 21 and from day 21 to day 28 in all groups (Figure 6B). There was no difference in ALP activity between group 1 and group 3 throughout the osteogenesis period. Expression was, however, higher in group 1 compared to group 2 on days 14 and 28 (Figure 6C).

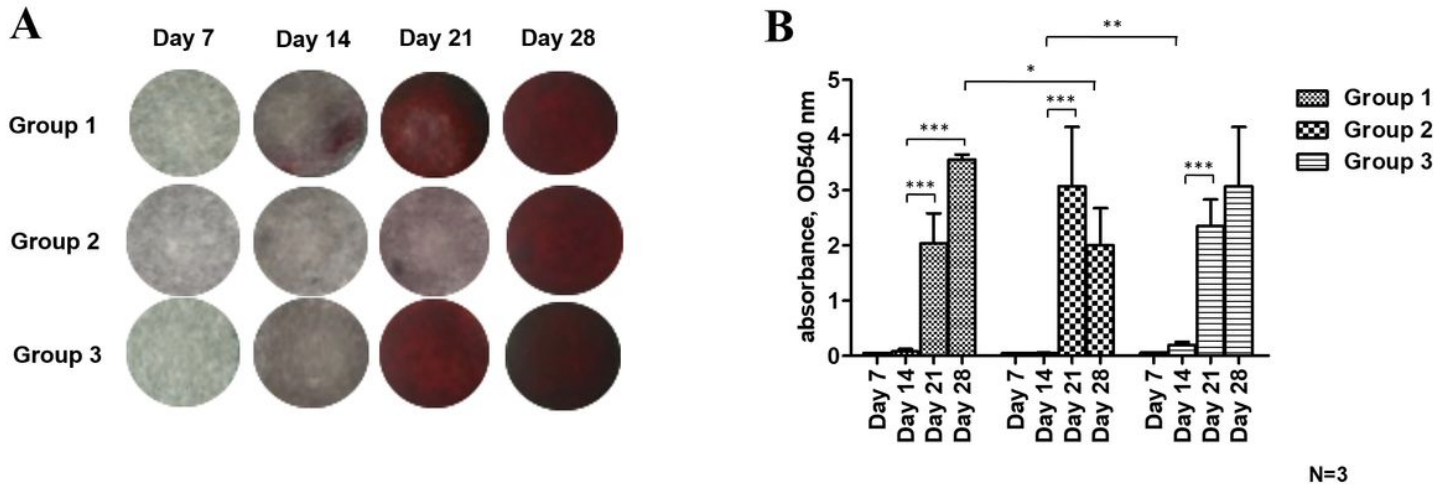

Figure 7

Alizarin red staining and activity Alizarin red staining (ARS) was visualized staining on day 21 in group 1 and group 3, and on day 28 in group 2 (Figure 7A). Using the ARS quantification assay, the absorbance value significantly increased from day 14 to day 21 in all three groups. On day 28, calcium deposition was significantly lower in group 2 compared to group 1. On day 14, calcium deposition was significant lower in group 2 compared to group 3 (Figure 7B).

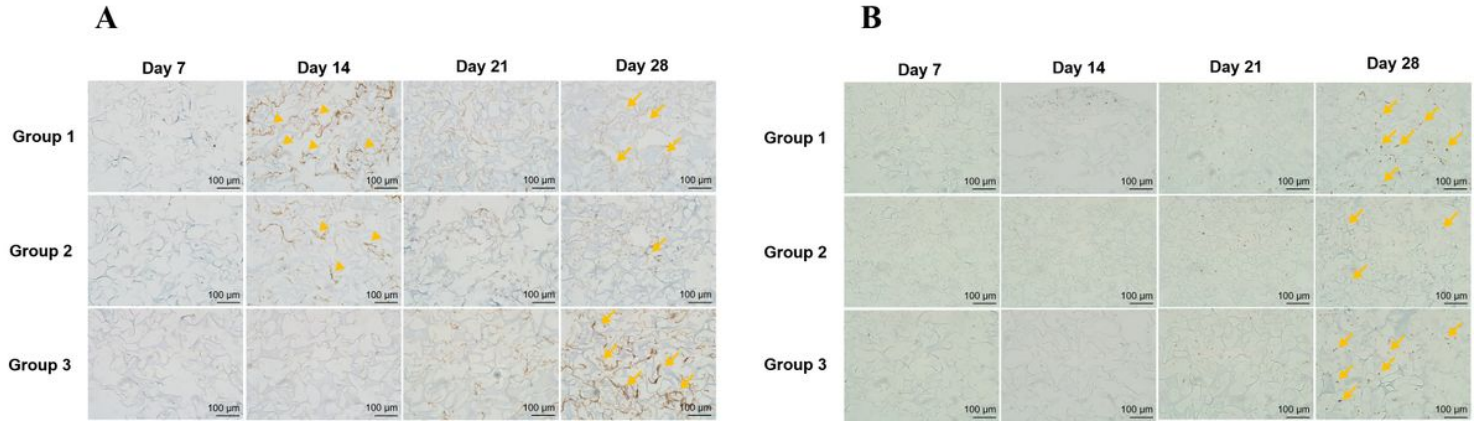

Figure 8

Immunohistochemistry of osteogenic related markers Immunohistochemistry for Col-I and OC was conducted to evaluate bone formation (Figure 8). On day 28, Col-I was more highly expressed in groups 1 and 3 compared to group 2. Col-I was detected as early as day 14 because the scaffold itself is highly composed of collagen (Figure 8A). Immunohistochemistry of OC was observed from day 21 in all three groups. On day 28, expression was significantly higher in group 1 and 3 than in group 2 (Figure 8B).